

Competition reactions of  $\text{Pt}(\text{dien})^{2+}$  with  $\text{XpG}$  ( $\text{X} = \text{A}, \text{C}, \text{T}$ ) indicated that the reactivity of  $\text{Pt}(\text{dien})^{2+}$  with the guanine base is influenced by the unplatinated  $\text{X}$ -bases.<sup>17</sup> The results suggest that the first platination step is controlled by the unplatinated base adjacent to the platinated guanine. In the present work, no difference was observed for the two isomers (*RS-1* and *RS-2*) produced from the reaction of  $\text{d}(\text{GpG})$  with  $\text{Pt}(\text{R,S-dach})^{2+}$ , whereas a significant difference was observed between the two isomers produced from the reaction of  $\text{Pt}(\text{R,S-dach})^{2+}$  with  $\text{d}(\text{ApG})$ .<sup>18</sup> The result of competition reactions between  $\text{Pt}(\text{R,R-dach})\text{Cl}_2$  and  $\text{Pt}(\text{R,S-dach})\text{Cl}_2$  with a common reactant  $\text{d}(\text{GpG})$  shows that  $\text{Pt}(\text{R,R-dach})(\text{d}(\text{GpG})\text{-N7,N7})$  appears to be a slightly predominant species, compared to  $\text{Pt}(\text{R,S-dach})(\text{d}(\text{GpG})\text{-N7,N7})$  (data not shown). However, no difference was observed between the amounts of *RS-1* and *RS-2*. These results suggest that the cyclohexane ring of  $\text{Pt}(\text{R,S-dach})^{2+}$  hardly impedes the approach of  $\text{d}(\text{GpG})$ . This may be attributed to the flexibility of both  $\text{Pt}(\text{R,S-dach})^{2+}$  and  $\text{d}(\text{GpG})$ .

Since the  $\text{-GpG-}$  sequence in DNA exists in a restricted environment compared to that of the dinucleotide,  $\text{d}(\text{GpG})$ , a significant difference might be provided for the reaction products between  $\text{Pt}(\text{R,S-dach})^{2+}$  and the  $\text{-GpG-}$  sequence in DNA. In fact, the ratio of the two isomers (*RS-1* and *RS-2*)—which are obtained from the enzymatic digestion<sup>3f,8</sup> of the reaction solution of  $\text{Pt}(\text{R,S-dach})^{2+}$  with DNA—is not equal (*RS-1:RS-2* = 0.63:0.37).<sup>7</sup> Molecular model inspection suggests that  $\text{Pt}(\text{R,S-}$

*dach*)<sup>2+</sup> after the first platination is situated inside of the DNA helix when the N7 site of the 3'G base binds to the same side of the *S*-carbon atom. Then, the 1:1 intermediate forms a chelate with the 5'G base (17-membered chelate ring) to yield *RS-2*. When the N7 site of the 3'G base binds to the same side of the *R*-carbon atom,  $\text{Pt}(\text{R,S-dach})^{2+}$  is oriented to the outside of the DNA helix. On the other hand, when the *S*-side of  $\text{Pt}(\text{R,S-dach})^{2+}$  binds to the 5'G base of the  $\text{-GpG-}$  sequence in DNA, *RS-1* is expected as the end product. In the reaction of  $\text{Pt}(\text{R,S-dach})^{2+}$  with  $\text{-GpG-}$  sequence in B-DNA, if the first platination to the 3'G base is preferred to that to the 5'G base, formation of *RS-1* might be superior to that of *RS-2*. The cyclohexane ring in the 1:1 intermediate of *RS-2* being situated inside of the DNA helix—seems to experience greater steric hindrance through the rotation about the Pt–N7 bond, and this may be a reason why the amounts of *RS-2* are less than those of *RS-1* in the case of the reaction of DNA. However, it remains unresolved which side of the guanine residue (3'G or 5'G) is preferred for the first platination. Whereas the dinucleotide  $\text{d}(\text{GpG})$  is a considerably flexible molecule, consequently, the same ratio of both isomers (*RS-1* and *RS-2*) is likely to be observed in the case of the reaction of  $\text{Pt}(\text{R,S-dach})^{2+}$  with  $\text{d}(\text{GpG})$ .

**Acknowledgment.** This work was supported in part by a Grant-in-Aid from the Ministry of Education, Science and Culture (No. 01101002) and from the Ministry of Health and Welfare of Japan. Prof. Dr. Jan Reedijk (Leiden University) is thanked for critical reading and valuable comments about the manuscript.

**Supplementary Material Available:** Figures S1 and S2, showing the pH–NMR titration curves of  $\text{Pt}(\text{R,R/S,S/R,S-dach})(\text{d}(\text{GpG})\text{-N7,N7})$  (2 pages). Ordering information is given on any current masthead page.

(18) The reaction gave two  $\text{Pt}(\text{R,S-dach})(\text{d}(\text{ApG})\text{-N7,N7})$  adducts, as is the case of the reaction between  $\text{d}(\text{GpG})$  and  $\text{Pt}(\text{R,S-dach})^{2+}$ . The ratio of the two adducts was 65:35, being calculated from the integration of the NMR spectrum.

Contribution from the Departament de Química Inorgànica, Universitat de Barcelona, Diagonal 647, 08028 Barcelona, Spain, Departament de Química Inorgànica, Facultat de Química, Universitat de València, Dr. Moliner 50, 46100 Burjassot, València, Spain, and Laboratoire de Chimie Inorganique, URA 420 CNRS, Université de Paris-Sud, 91405 Orsay, France

## Oxalato-Bridged and Related Dinuclear Copper(II) Complexes: Theoretical Analysis of Their Structures and Magnetic Coupling

Santiago Alvarez,<sup>\*,1a</sup> Miguel Julve,<sup>\*,1b</sup> and Michel Verdaguer<sup>\*,1c</sup>

Received December 14, 1989

A theoretical analysis of the structural variations found for dinuclear Cu(II) complexes with oxalato and related polynuclear bridging ligands and their influence on the magnitude of the magnetic exchange interactions is presented in this paper. The family of compounds studied can be represented by the general formula  $[(\text{AA})\text{Cu}(\mu\text{-C}_2\text{O}_4)\text{Cu}(\text{AA})]\text{X}_n$ , where AA can be a chelating ligand like 2,2'-bipyridine (bpy) or tetramethylethylenediamine (tmen), and X is a counteranion or a solvent molecule. Three types of distortions from an ideal square-planar geometry around the copper atoms are considered: (1) the removal of the copper ions from the ligands' plane; (2) a twist of the square planar  $\text{A}_2\text{CuO}_2$  cores toward a tetrahedral geometry by rotation of the AA ligand; (3) folding of the  $\text{A}_2\text{Cu-ox-CuA}_2$  skeleton through the O–O hinges and axial coordination of X. An evaluation of second-order Jahn–Teller distortions through the analysis of orbital topologies and atomic electronegativities is presented, which might be helpful in predicting how stable a distorted molecule is relative to the undistorted one, as well as the relative extent for such distortions in a series of related structures.

In the last few years, there has been a great deal of interest in the synthesis and magnetic coupling of transition-metal atoms with polyatomic bridging ligands.<sup>2</sup> A sound theoretical interpretation of the factors contributing to the magnetic coupling in dinuclear complexes is now available thanks to the classical work of Hay, Thibault, and Hoffmann<sup>3</sup> and later contributions from

Kahn and co-workers.<sup>4</sup> However, the wide range of structural variations found for dinuclear Cu(II) complexes with oxalato and similar bridging ligands and their influence on the magnitude of the magnetic interactions have not been considered in detail previously, and we feel a theoretical analysis of such features is in order.

A number of dinuclear copper complexes with oxalato bridge, which can be represented by the general formula  $[(\text{AA})\text{Cu}(\mu\text{-C}_2\text{O}_4)\text{Cu}(\text{AA})\text{X}_n]$ , have been structurally characterized in the last few years.<sup>5–8</sup> In these complexes, AA is a chelating ligand,

(1) (a) Universitat de Barcelona. (b) Universitat de València. (c) Université de Paris-Sud.

(2) Willett, R. D.; Gatteschi, D.; Kahn, O., Eds. *Magneto-Structural Correlations in Exchange-Coupled Systems*; NATO ASI Series 140; D. Reidel: Dordrecht, The Netherlands, 1985.

(3) Hay, P. J.; Thibault, J. C.; Hoffmann, R. *J. Am. Chem. Soc.* **1975**, *97*, 4884.

(4) See, e.g.: Kahn, O. *Angew. Chem., Int. Ed. Engl.* **1985**, *24*, 834, and references therein.

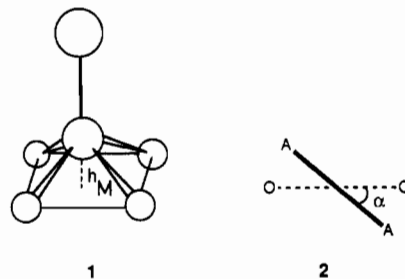
**Table I.** Structural and Magnetic Data for Dinuclear, Oxalato- and Tetrathiooxalato-Bridged Complexes of the Type [(AA)M( $\mu$ -C<sub>2</sub>Y<sub>4</sub>)M(AA)]X<sub>2</sub> (M = Cu, Ni)

AA	X <sup>a</sup>	donor set <sup>b</sup>	$h_M$ , <sup>c</sup> Å	$\gamma$ , deg	$\alpha$ , deg	$d_{CC}$ , Å	$J$ , cm <sup>-1</sup>	ref
Cu-Oxalato Complexes								
tmen	ClO <sub>4</sub> <sup>d</sup>	O <sub>2</sub> N <sub>2</sub> O	0.18	8.4	4.8	1.54 (1)	-385	7
			0.15	12.1	6.3	1.56 (1)		
bpy	NO <sub>3</sub>	O <sub>2</sub> N <sub>2</sub> O	0.10	3.2	4.4	1.553 (4)	-385	5, 6
bpy	ClO <sub>4</sub>	O <sub>2</sub> N <sub>2</sub> O (O)	0.17	11.0	1.0	1.532 (5)	-360	6
phen	NO <sub>3</sub>	O <sub>2</sub> N <sub>2</sub> O	0.27	16.8	3.3	1.533 (4)	-330	8
bpy	BF <sub>4</sub>	O <sub>2</sub> N <sub>2</sub> O	0.16	10.4	7.2	1.533 (5)	-385	6
bpy	PF <sub>6</sub>	O <sub>2</sub> N <sub>2</sub> F (F)	0.08	3.2	0	1.538 (5)	-385	6
bpy <sup>e</sup>	Cl	O <sub>2</sub> N <sub>2</sub> Cl	0.37	15.0	4.3	1.526 (6)	-330	6
bzpm <sup>f</sup>	PF <sub>6</sub>	O <sub>2</sub> N <sub>2</sub> O	0.19	8.8	0.0	1.507 (16)	-349	12
mpz <sup>g</sup>	NO <sub>3</sub>	O <sub>2</sub> N <sub>2</sub> O	0.24	13.9	5.3	1.52 (2)	-402	13
Ni-Oxalato Complexes								
cyclam	NO <sub>3</sub>	O <sub>2</sub> N <sub>4</sub>	0.0	2.8	5.8	1.536 (7)	-39	14
PR <sub>3</sub> ,Me		O <sub>2</sub> PC	0.04	3.0	0.3	1.532 (5)		15
Me <sub>2</sub> cyclen	ClO <sub>4</sub>	O <sub>2</sub> N <sub>4</sub>	0.02	0.8	0.3	1.547 (5)	-35	16
tn <sup>h</sup>	ClO <sub>4</sub>	O <sub>2</sub> N <sub>4</sub>	0.02	2.6	1.1	1.570 (18)	-36.4	17
Tetrathiooxalato Complexes								
PEt <sub>3</sub> ,	Cl	S <sub>6</sub> PCl	0.19	8.0	3.0	1.34 (4)		18
C <sub>3</sub> OS <sub>4</sub>		S <sub>4</sub>	0.03	14.5	25.2	1.467 (10)	<-800	19
(PPh <sub>3</sub> ) <sub>2</sub>		S <sub>2</sub> P <sub>2</sub>	0.19	<i>f</i>	44.5	1.531 (8)		20

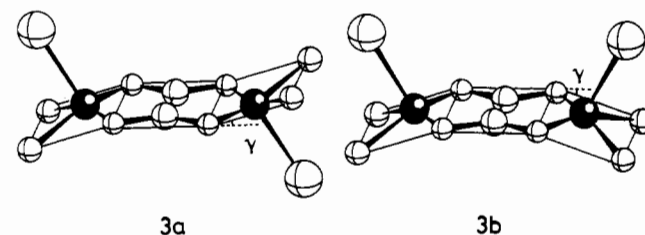
<sup>a</sup>Counteranion. <sup>b</sup>The four first atoms are those in the basal plane, the fifth corresponds to the apical position, and the atom in parentheses corresponds to a sixth, loosely bound, axial ligand. <sup>c</sup>The height of the M atom above the basal (Y<sub>2</sub>A<sub>2</sub>) plane. <sup>d</sup>The two sets of structural data for this compound correspond to the two nonequivalent crystallographic positions. <sup>e</sup>This compound presents a boat conformation **3b**. All others are in the chair conformation **3a**. <sup>f</sup>Distortion too large for this angle to be significant. <sup>g</sup>Key: bzpm = bromazepam; tn = 1,3-diaminopropane, cyclam = 1,4,8,11-tetraazacyclotetradecane; cyclen = 1,4,7,10-tetraazacyclododecane; mpz = mepirizole.

typically a diamine like 2,2'-bipyridine (bipy) or tetramethylethylenediamine (tmen), and X is a counteranion or a solvent molecule. In most cases, the copper ions present a square-pyramidal structure with two oxygen atoms of the oxalato bridge and two nitrogen atoms of the diamine occupying the base of the pyramid and the counteranion or a solvent molecule occupying the axial coordination site. Some compounds present an additional bond to X, giving rise to pseudooctahedral coordination; however, this bond is very weak, and we can consider those compounds as approximately square pyramidal. Although there are some compounds in which the square pyramids are not connected by the oxalato bridge through the basal plane or some that have a trigonal-bipyramidal geometry around the copper atoms,<sup>9-11</sup> we will limit the present study to dinuclear complexes with the copper atoms in a tetragonal environment (i.e., square planar, square pyramidal, or pseudooctahedral) bridged by an oxalato ligand through their equatorial planes.

If we take idealized square-planar ML<sub>4</sub> fragments as a starting point for the description of the geometries of these compounds, the experimental structures can be described by the following distortions: (a) the four donor atoms in the basal plane are not perfectly planar, and the deviation from an ideally planar A<sub>2</sub>O<sub>2</sub> donor set can be described by means of the twist angle between the A-A vector and the oxalato plane ( $\alpha$ , **2**); (b) the coordination of a fifth ligand X results in a square pyramidal coordination sphere, with the metal atom displaced out of the equatorial plane towards the axial ligand ( $h_M$ , **1**); (c) the base of the pyramid and



the oxalato bridge are not coplanar, giving rise to either a "chair" (**3a**) or a "boat" (**3b**) conformation, the angles formed between



these two planes being represented by  $\gamma$ . The values of  $h_M$ ,  $\alpha$ , and  $\gamma$ , obtained from the experimental data of Cu and Ni complexes in the literature, are shown in Table I.

All the oxalato-bridged dinuclear Cu(II) compounds of structural type **3** studied so far have been found to be antiferromagnetic. A remarkable feature of their magnetic behavior is that the magnitude of the coupling constant appears to be only

- Julve, M.; Faus, J.; Verdager, M.; Gleizes, A. *J. Am. Chem. Soc.* **1984**, *106*, 8306.
- Julve, M.; Faus, J.; Verdager, M.; Gleizes, A.; Kahn, O. To be published.
- Julve, M.; Verdager, M.; Gleizes, A.; Philoche-Levisalles, M.; Kahn, O. *Inorg. Chem.* **1984**, *23*, 3808.
- Bencini, A.; Fabretti, A. C.; Zanchini, C.; Zannini, P. *Inorg. Chem.* **1987**, *26*, 1445.
- Felthouse, T. R.; Laskowski, E. J.; Hendrickson, D. N. *Inorg. Chem.* **1977**, *16*, 1077.
- Curtis, N. F.; McCormick, I. R. N.; Waters, T. N. *J. Chem. Soc., Dalton Trans.* **1973**, 1537.
- The structure of the nitrite salt described in ref 6 does not correspond to base-connected square pyramids.
- Real, J. A.; Borrás, J.; Solans, X.; Font-Altaba, M. *Transition Met. Chem.* **1987**, *12*, 254.
- Soto, L.; Garcia, J.; Escriva, E.; Legros, J.-P.; Tuchagues, J.-P.; Dahan, F.; Fuentes, A. *Inorg. Chem.* **1989**, *28*, 3378.
- Battaglia, L. P.; Bianchi, A.; Bonamartini Corradi, A.; Garcia-España, E.; Micheloni, M.; Julve, M. *Inorg. Chem.* **1988**, *27*, 4174.
- Klein, H.-F.; Wiemer, T.; Menu, M.-J.; Dartiguenave, M.; Dartiguenave, Y. *Inorg. Chim. Acta* **1988**, *154*, 21.
- Bencini, A.; Bianchi, A.; Garcia-España, E.; Jeannin, Y.; Julve, M.; Marcelino, V.; Philoche-Levisalles, M. *Inorg. Chem.* **1990**, *29*, 963.
- Ribas, J.; Monfort, M.; Díaz, C.; Solans, X. *An. Quim., Ser. B* **1988**, *84B*, 186.
- Cetinkaya, B.; Hitchcock, P. B.; Lappert, M. F.; Pye, P. L.; Shaw, D. B. *J. Chem. Soc., Dalton Trans.* **1979**, 434.
- Vicente, R.; Ribas, J.; Alvarez, S.; Seguí, A.; Solans, X.; Verdager, M. *Inorg. Chem.* **1987**, *26*, 4004.

- Hansen, L. K.; Sieler, J.; Strauch, P.; Dietzsch, W.; Hoyer, E. *Acta Chem. Scand., Ser. A* **1985**, *A39*, 571.

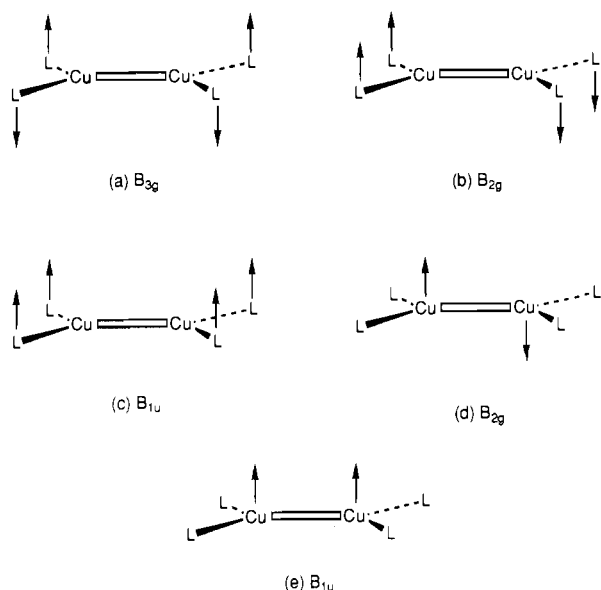


**Figure 1.** Some distortion modes for a planar (AA)Cu( $\mu$ -C<sub>2</sub>Y<sub>4</sub>)Cu(AA) framework.

slightly sensitive to the important structural differences, with values of  $J$  between  $-330$  and  $-402$  cm<sup>-1</sup>. Related di- and trinuclear oxamato- and oxamidato-bridged complexes have been also synthesized and appear to behave similarly.<sup>21-24</sup>

Recently, analogous dinuclear complexes with bridging tetrathiooxalato group of the type [A<sub>2</sub>M-( $\mu$ -C<sub>2</sub>S<sub>4</sub>)-MA<sub>2</sub>] have been reported.<sup>18-20</sup> In these compounds, the metal atom presents an approximate square-planar coordination, with varying degrees of twisting towards a tetrahedral geometry (represented by the angle  $\alpha$ , Table I). A theoretical analysis<sup>19</sup> showed that the driving force for such distortion ( $B_{3g}$  in Figure 1a) is a second-order Jahn-Teller effect, resulting in a lengthening of the C-C bond of C<sub>2</sub>S<sub>4</sub> for the cases with stronger deviation from planarity of the metal environment. The  $B_{2g}$  and  $B_{1u}$  distortions (Figure 1b,c) would lead to chair and boat conformations analogous to those found in the pentacoordinate oxalato-bridged copper complexes, but they were found to be not stabilizing. As can be seen in Table I, both the carbon-carbon bond distance and the degree of twisting of the basal plane,  $\alpha$ , present wider ranges for the tetrathiooxalato- than for the oxalato-bridged compounds. The coordination of a fifth ligand in an axial position, the folding of the basal plane around the O-O hinge ( $\gamma$ ), and the displacement of the metal atom out of the basal plane have been previously detected in oxalato but not in tetrathiooxalato complexes. In Table I, it can be seen that folding of the basal plane is also present in tetrathiooxalato complexes.

In the following, we shall discuss some particular aspects of the second-order Jahn-Teller distortions (SOJT), in search of the qualitative concepts that may allow us to explain the structural differences between families of dinuclear complexes with different polyatomic bridges, such as oxalato, tetrathiooxalato, bipyrimidine, benzoquinone, and others.

### Second-Order Jahn-Teller Distortions: Analysis of Orbital Topologies and Atomic Electronegativities

It is well-known that when a molecule in a particular geometry has an empty MO close in energy to an occupied one, a symmetry decrease may allow mixing of both orbitals, leading to a net stabilization. This is a result of the second-order term in the Jahn-Teller evaluation of the energetics of molecular distortions<sup>25</sup>

(abbreviated SOJT from here on). The symmetry prescription for such distortions is that the normal mode representing the nuclear displacements must belong to the same symmetry species as the direct product of those of the empty and occupied molecular orbitals. The symmetry analysis tells us when a particular distortion mode can stabilize a molecule, but not how stable the distorted molecule will be compared to the undistorted one or which factors affect the extent of the distortion. An understanding of the factors contributing to the SOJT distortions should allow us to predict how to control them through chemical substitutions.

Let us consider two molecular orbitals of a particular molecule:  $\Phi_1$  and  $\Phi_2$  with energies  $E_1$  and  $E_2$ , respectively, belonging to different symmetry species. These can be expressed as linear combinations of atomic orbitals:

$$\begin{aligned}\Phi_1 &= \sum_{\mu} c_{1\mu} \chi_{\mu} \\ \Phi_2 &= \sum_{\nu} c_{2\nu} \chi_{\nu}\end{aligned}\quad (1)$$

If the molecule is distorted to a nuclear configuration of lower symmetry, such that  $\Phi_1$  and  $\Phi_2$  become of the same symmetry species, they are then allowed to interact. This interaction can be studied by means of perturbation theory, as usually done for the interaction of two atomic orbitals.<sup>26</sup> The first order term can only be nonzero if the ground state is degenerate,<sup>25</sup> and for the present dinuclear Cu(II) compounds, it does not affect the planar (AA)Cu( $\mu$ -C<sub>2</sub>O<sub>4</sub>)Cu(AA) skeleton. The second-order energy terms are of the form

$$\begin{aligned}E_1'' &= \frac{H_{12}H_{21}}{E_1 - E_2} \\ E_2'' &= \frac{H_{12}H_{21}}{E_2 - E_1}\end{aligned}\quad (2)$$

where  $H_{12} = \langle \Phi_1 | \mathbf{H}' | \Phi_2 \rangle$ ,  $\mathbf{H}'$  being the perturbation Hamiltonian. The wave functions for the distorted molecule are

$$\begin{aligned}\Psi_1 &= \Phi_1 + \frac{\langle \Phi_1 | \mathbf{H}' | \Phi_2 \rangle}{E_1 - E_2} \Phi_2 \\ \Psi_2 &= \Phi_2 + \frac{\langle \Phi_2 | \mathbf{H}' | \Phi_1 \rangle}{E_2 - E_1} \Phi_1\end{aligned}$$

Using the Wolfsberg-Helmholz approximations<sup>27</sup> for the above integrals, i.e.

$$H_{12} = (K/2)S_{12}(H_{11} + H_{22})\quad (3)$$

where  $S_{12}$  is the overlap integral of the unperturbed wave functions  $\langle \Phi_1 | \Phi_2 \rangle$  in the distorted geometry. The second-order stabilization of  $\Psi_1$  relative to  $\Phi_1$  then becomes

$$E_1'' = \frac{K^2 S_{12}^2 (H_{11} + H_{22})^2}{4(E_1 - E_2)}\quad (4)$$

The energy difference in the denominator is typical of perturbational expressions. The overlap dependence deserves further comment. It is clear that the overlap can be nonzero only if  $\Phi_1$  and  $\Phi_2$  are of the same symmetry, as stated above. The next question is, when  $S_{12}$  is nonzero, how large is it? In order to answer this question, we can expand  $S_{12}$  in terms of orthonormalized atomic orbitals, by means of eq 1:

$$S_{12} = \sum_{\mu, \nu} c_{1\mu} c_{2\nu} \langle \chi_{\mu} | \chi_{\nu} \rangle\quad (5)$$

(21) Ribas, J.; García, A.; Costa, R.; Monfort, M.; Alvarez, S.; Zanchini, C.; Solans, X.; Domenech, M. V. Submitted for publication.

(22) Ribas, J. Personal communication.

(23) Verdager, M.; Kahn, O.; Julve, M.; Gleizes, A. *Nouv. J. Chim.* **1985**, *9*, 325.

(24) Lloret, F.; Julve, M.; Faus, J.; Journaux, Y.; Philoche-Levisalles, M.; Jeannin, Y. *Inorg. Chem.* **1989**, *28*, 3702.

(25) (a) Jahn, H. A.; Teller, E. *Proc. R. Soc. London* **1937**, *A161*, 220. (b) Bartell, L. S. *J. Chem. Educ.* **1968**, *45*, 754. (c) Pearson, R. G. *J. Am. Chem. Soc.* **1969**, *91*, 4947. (d) Albright, T. A.; Burdett, J. K.; Whangbo, M.-H. *Orbital Interactions in Chemistry*; Wiley: New York, 1985. (e) Bersuker, I. B. *The Jahn-Teller Effect and Vibronic Interactions in Modern Chemistry*, Plenum Press: New York, 1984.

(26) Hoffmann, R. *Acc. Chem. Res.* **1971**, *4*, 1.

(27) Wolfsberg, M.; Helmholz, L. *J. Chem. Phys.* **1952**, *20*, 837.

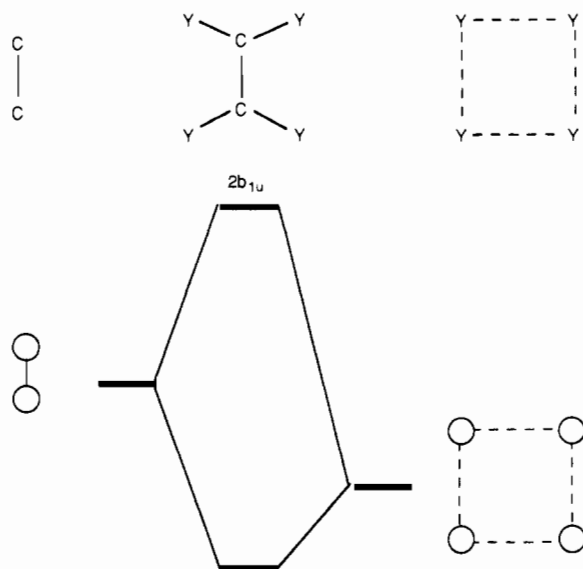


**Figure 2.** Diagram for the interaction between the  $\pi$ -bonding orbital of the central C-C fragment and the outer donor atoms in  $C_2Y_4$  ligands.

If we represent the overlap integrals  $\langle \chi_\mu | \chi_\nu \rangle$  in eq 5 by  $S_{\mu\nu}$  and separate the diagonal terms, recalling that  $S_{\mu\mu} = 1$  (normalization condition)

$$S_{12} = \sum_{\mu} c_{1\mu} c_{2\mu} + \sum_{\mu \neq \nu} c_{1\mu} c_{2\nu} S_{\mu\nu} \quad (6)$$

Hence,  $S_{12}$  depends on the values of the overlap integrals between the atomic orbitals,  $S_{\mu\nu}$ , and also on the values of the coefficients in the LCAO's of the undistorted molecule.

Let us take a closer look at the different contributions to  $S_{12}$  in eq 6. Since the first term is constant, changes in the value of  $S_{12}$  upon distortion are only associated with the second term. Furthermore, in the second term, all the integrals  $S_{\mu\nu}$  with  $\mu$  and  $\nu$  centered on the same atom are zero because of the orthogonality of the atomic orbitals.

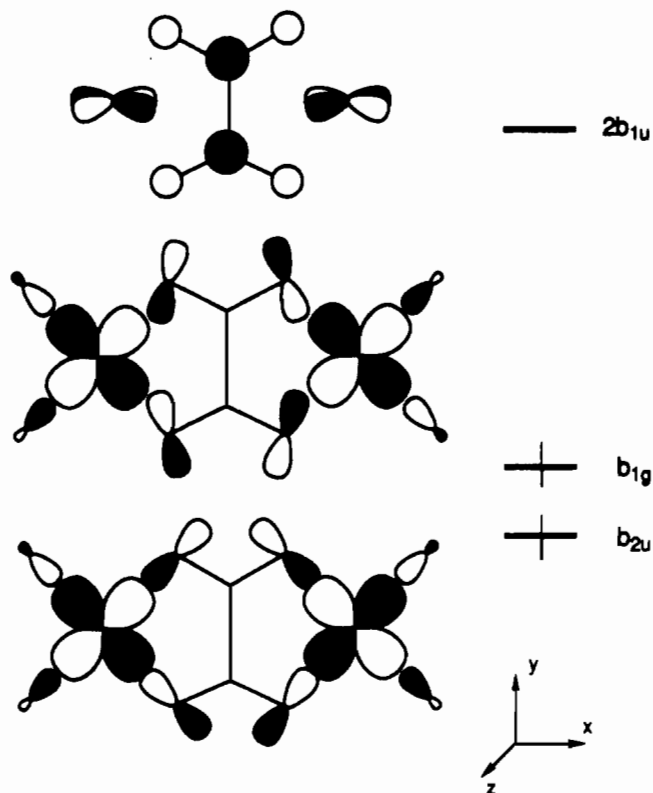
Therefore, changes in  $S_{12}$  and, consequently, in the stabilization energy (eq 4) are due to the changes in the overlaps  $S_{\mu\nu}$  between atomic orbitals centered on different atoms. The largest variations in such integrals correspond to  $\mu$  and  $\nu$  on bonded atoms whose relative positions change upon distortion. Atoms at two-bond distances may also be important if the distortion mode makes them approach each other.

Two factors affect the values of these overlap integrals as the molecule is distorted: (i) changes in bond angles, governed by simple rules that have been systematized within the "angular overlap model" (AOM),<sup>28</sup> and (ii) changes in interatomic distances. These two factors have been well-studied in most simple molecules through their Walsh diagrams.<sup>29</sup> On the other hand, such integrals appear in eq 6 multiplied by  $c_{1\mu} c_{2\nu}$ , and therefore, the coefficients are as important as the changes in overlap in determining the stabilization energy.

In summary, in order to obtain substantial stabilization through a SOJT distortion,  $\Phi_1$  and  $\Phi_2$  must have large coefficients on neighboring atoms. Needless to say, the atomic orbitals centered on atoms whose relative positions change upon distortion are the only ones whose overlap change significantly upon distortion. As a consequence, one can easily predict the parts of a molecule at which a SOJT distortion is likely to appear simply by looking at the localization of the high-energy filled and low-energy empty orbitals (typically the HOMO and LUMO, but not necessarily so).

### Molecular Orbitals and the $B_{3g}$ Twisting Distortion

We will not discuss in detail in this paper the molecular orbitals of the studied compounds but will consider only the three valence orbitals of the planar model compound  $[(H)_2Cu(\mu-C_2O_4)Cu(H)_2]^{2-}$  represented in 4. There, the lowest two orbitals (HOMO



4

and LUMO) are the in-phase and out-of-phase combinations of the  $d_{xy}$  (Cu) orbitals, mixed with the lone-pair orbitals of the oxalato bridge of the same symmetry species,  $b_{2u}$  and  $b_{1g}$  ( $D_{2h}$  point group). The third orbital ( $2b_{1u}$ ) is centered on the bridging ligand, with  $\pi_{CC}$  and  $\pi_{CS}^*$  character. The reader may find in the literature a more detailed description of the molecular orbitals of square-pyramidal  $ML_5$  fragments.<sup>25d,38</sup> Also discussions on the molecular orbitals of planar  $C_2Y_4^{2-}$  ions and their interaction with  $ML_n$  fragments can be found in previous publications.<sup>3,19,23,30</sup> The main difference between the orbital levels shown in 4 for the oxalato compound and the corresponding ones for a tetrathiooxalato derivative<sup>19</sup> is that  $2b_{1u}$  appears above  $b_{2u}$  and  $b_{1g}$  for the oxalato complex because of the longer C-C distance. This change in orbital ordering is not important for the study of the SOJT effect since mixing of two orbitals depends on the absolute value and not on the sign of their energy difference.

Following the reasoning of the previous section, we see that a SOJT distortion allowing mixing of  $2b_{1u}$  and  $b_{2u}$  ( $B_{3g}$  distortion mode<sup>19</sup>) or of  $2b_{1u}$  and  $b_{1g}$  ( $A_u$  distortion mode) could stabilize the dinuclear compound if (a) the energy difference between  $2b_{1u}$  and  $b_{2u}$  (or  $b_{1g}$ ) is small and (b) the orbitals being mixed have large coefficients on the atoms whose relative positions change upon distortion. A look at the MO topologies in 4 tells us that such a distortion may affect only the positions of the  $CuL_2$  fragments relative to the oxalato bridge.

The extent of second-order mixing and, consequently, the degree of stabilization achieved through the  $B_{3g}$  distortion, depends on the squares of the coefficients with which the atomic orbitals of the Cu and Y atoms participate in the  $2b_{1u}$  and  $b_{2u}$  molecular orbitals (eqs 4 and 6). Since we want to study the effect of different bridges while keeping the same  $CuA_2$  fragments, we need only consider the differences in coefficients on the Y atoms. Both

(28) (a) Burdett, J. K. *Molecular Shapes*; J. Wiley: New York, 1980. (b) Burdett, J. K. *Adv. Inorg. Chem. Radiochem.* **1978**, *21*, 113. (c) Larsen, E. M.; LaMar, G. N. *J. Chem. Educ.* **1974**, *51*, 633. (d) Gerloch, M.; Slade, R. C. *Ligand Field Parameters*; Cambridge University Press: Cambridge, England, 1973.

(29) Gimarc, B. M. *Molecular Structure and Bonding*; Academic Press: New York, 1976.

(30) Alvarez, S.; Vicente, R.; Hoffmann, R. *J. Am. Chem. Soc.* **1985**, *107*, 6253.

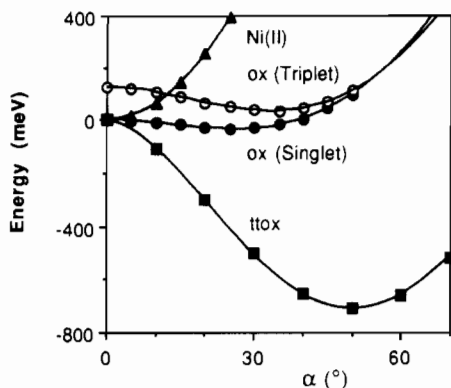


**Figure 3.** One-electron stabilization energy as a function of the  $B_{3g}$  twisting distortion  $\alpha$  for model dinuclear compounds:  $[(H)_2Cu(\mu-C_2O_4)Cu(H)_2]^{2-}$  in its singlet (open circles) and triplet (triangles) configurations,  $[(H)_2Cu(\mu-C_2S_4)Cu(H)_2]^{2-}$  in its singlet configuration (squares), and  $[(H)_2Cu(\mu-C_2O_4)Cu(H)_2]$ , a model for the Ni(II) dinuclear complexes (filled circles). The zero of energy has been arbitrarily chosen at  $\alpha = 0^\circ$  for all cases.

the  $\sigma$ -type lone pair and the  $\pi_{CC}$  orbitals of the  $C_2Y_4$  entity that contribute to  $b_{2u}$  and  $2b_{1u}$  can be described as resulting from the interaction of a central  $C_2$  unit with a rectangular array of the four Y donor atoms, as schematically shown in Figure 2 for Y = S. If more electronegative oxygen atoms are substituted for the sulfur ones in  $C_2Y_4$ , the energy match between the  $C_2$  and  $Y_4$  orbital becomes poorer, and consequently, both  $n_\sigma$  and  $\pi_{CC}$  will be more localized on the carbon atoms, leading to poorer interactions with the metal d orbitals and smaller coefficients at Y for the  $b_{2u}$  and  $2b_{1u}$  molecular orbitals. We can thus conclude that the extent of the  $B_{3g}$  SOJT distortion must be smaller for the complexes having the more electronegative donor atoms; i.e., smaller distortions are to be expected for the oxalato-bridged than for the tetrathiooxalato-bridged complexes.

The calculated one-electron energy curves for both the singlet and triplet configurations of our model dinuclear complex  $A_2Cu(\mu-C_2Y_4)CuA_2$  (Figure 3; Y = O, L = H<sup>-</sup>) show that the  $B_{3g}$  distortion stabilizes such hypothetical molecules (see Appendix for computational details). Notice that we cannot calculate the energy difference between singlet and triplet states due to the neglect of bielectronic interactions at the extended Hückel level, and the one-electron energy curves of Figure 3 are plotted only to show that the stabilization achieved through the  $B_{3g}$  distortion is similar in both cases. The net stabilization calculated for our model copper-oxalato compound upon rotation is a small 0.1 eV, compared to 0.5 eV for the tetrathiooxalato bridge, in agreement with the above qualitative predictions. The minima for such model calculations are found at  $\sim 30^\circ$  for  $C_2O_4$  and at  $\sim 50^\circ$  for  $C_2S_4$  (Figure 3). The available structural information is consistent with these results, since the  $B_{3g}$  rotation is indeed present in the oxalato complexes studied here only as a minor effect (Table I). An additional result of the SOJT mixing should be a weakening of the C-C bond with the angle  $\alpha$ .<sup>19</sup> The differences in electronegativity between O and S are also reflected in the range of the experimental C-C distances as shown in Figure 4.

For oxalato-bridged Ni(II) dinuclear complexes, with two less electrons per dinuclear unit, the ground state is experimentally found to be a low-spin configuration.<sup>14-17</sup> In such a case, the  $b_{2u}$  and  $b_{1g}$  orbitals in **3** should be empty, and the SOJT distortion  $B_{3g}$  is not expected to be operative. Therefore, the total one-electron energy for  $[(H)_2Cu(\mu-C_2O_4)Cu(H)_2]$  (Figure 3), a model for the isoelectronic Ni(II) complexes, shows a minimum for the planar conformation (i.e.,  $\alpha = 0^\circ$ ) (Figure 3), in good agreement with the structural data (Table I). On the other hand, triplet or quintet states, thermally populated at room temperature, have the  $b_{2u}$  and  $b_{1g}$  orbitals occupied and contribute to the small twisting observed in some cases.

Now that our simple qualitative analysis of the molecular orbitals has been shown to match with both calculations and experimental data, we can try to make our study more general

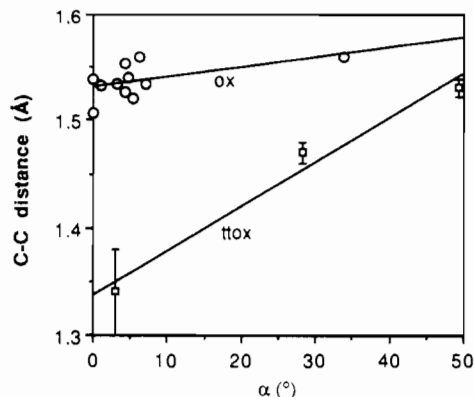


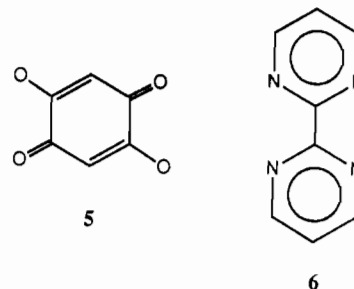
**Figure 4.** Plot of the experimental C-C bond distances of the  $C_2Y_4$  bridge as a function of the twisting angle  $\alpha$  for oxalato (Y = O) and tetrathiooxalato (Y = S) dinuclear complexes (see Table I for references). Least-squares lines are drawn only to show the trends.

**Table II.** Structural and Magnetic Data for Dinuclear, Bipyrimidine- and Benzoquinone-Bridged Complexes

$X^a$	donor set <sup>a</sup>	$\gamma$ , deg	$\alpha$ , deg	$d_{CC}$ , Å	$J$ , cm <sup>-1</sup>	ref
Bipyrimidine-Cu(II) Complexes						
Cl	$N_2Cl_2Cl_2$	23.7	4.4	1.472 (3)	-225	36
Br	$N_2Br_2Br_2$	2.2	3.6	1.470 (7)	-236	36
NCO	$N_2N_3O$	8.4	8.2	1.450 (9)	-198	35
NCS	$N_2N_2S_2$	0.7	1.1	1.461 (10)	-231	35
			0.6	1.475		
$NO_3^b$	$N_2O_4$			1.432 (8)	-191	34
$ClO_4$					-62	37
Benzoquinone-Cu(II) Complex						
	$O_2N_2O$	8.9	0.7		-25.9	31

<sup>a</sup>See explanations in Table I. <sup>b</sup>The octahedron is distorted in this compound due to the bidentate nature of  $NO_3^-$ .

by looking at different chemical modifications of the bridging ligand. A straightforward modification of the bridge consists in the extension of the intervening carbonaceous skeleton, as in the benzoquinone (**5**) derivatives<sup>31-33</sup> or bipyrimidine (**6**) complex-



es.<sup>34-37</sup> The main result of such an extension is an increased delocalization of the donor orbitals, i.e., decreased values of the coefficients which are responsible for the twisting distortion, resulting in a decreased importance of the  $B_{3g}$  distortion. Calculations on dinuclear Cu(II) complexes with such bridging ligands predict them to be practically planar ( $\alpha < 1^\circ$ ). The experimental values of  $\alpha$  in Table II agree with the predicted effect for the extension of the bridge.

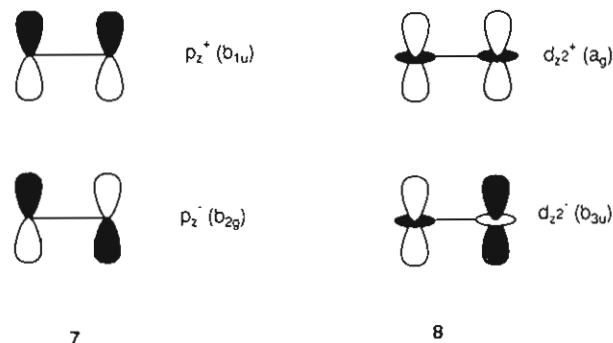
#### Bending of the Basal Plane around the O-O Hinge

The bending of the base of the square pyramid away from the oxalato plane is a characteristic structural feature of the studied

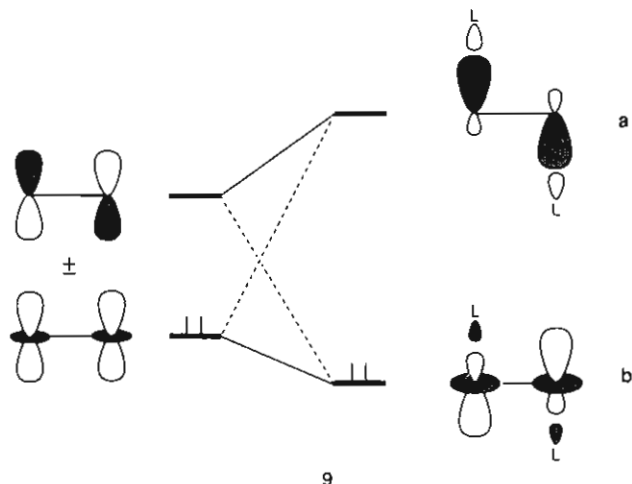
- (31) Tinti, F.; Verdager, M.; Kahn, O.; Savariault, J.-M. *Inorg. Chem.* **1987**, *26*, 2380.  
 (32) Verdager, M.; Michalowicz, A.; Girerd, J. J.; Alberding, N.; Kahn, O. *Inorg. Chem.* **1980**, *19*, 3271.  
 (33) Pierpont, C. G.; Francesconi, L. C.; Hendrickson, D. N. *Inorg. Chem.* **1977**, *16*, 2367.  
 (34) De Munno, G.; Bruno, G. *Acta Crystallogr.* **1984**, *C40*, 2030.  
 (35) Julve, M.; De Munno, G.; Verdager, M. Unpublished results.  
 (36) Julve, M.; De Munno, G.; Bruno, G.; Verdager, M. *Inorg. Chem.* **1988**, *27*, 3160.  
 (37) Julve, M.; De Munno, G. Unpublished results.

Cu(II) compounds. In the following, we will try to look for the orbital reasons of such behavior and will try to find out whether the bending has any effect on other structural parameters or on the magnetic behavior. Let us still consider our hypothetical planar  $[(AA)Cu(\mu\text{-ox})Cu(AA)]$  molecule (i.e., with no  $B_{3g}$  distortion) in order to make things clearer. The frontier orbitals 4 can account only for the rotations like  $B_{3g}$ , but not for the bending, actually a major structural feature for most square-pyramidal oxalato-bridged complexes.

In fact, we need to consider the bonding with the fifth ligand to account for such bending. How can the planar  $[(AA)Cu(\mu\text{-ox})Cu(AA)]$  skeleton interact with the  $\sigma$ -donor orbitals of the apical ligand? Both  $p_z$  (7) and  $d_{z^2}$  (8) metal orbitals have the right



topology. In the planar moiety, the  $p_z$  and  $d_{z^2}$  orbitals cannot mix because of the existence of a symmetry plane. If the symmetry plane were lost, mixing of both orbitals would result in the formation of hybrid orbitals best suited to overlap with the  $\sigma$ -donor orbitals of the incoming apical ligands as schematically shown in 9. It is straightforward to deduce that the distortion that allows



mixing of  $p_z$  and  $d_{z^2}$  orbitals must belong to the  $B_{2g}$  or  $B_{1u}$  irreducible representations of the  $D_{2h}$  point group. These are in fact the bending motions leading to chair or boat conformations (Figure 1b,c), or the pyramidalization<sup>38</sup> of the copper atom (Figure 1d,e), which are actually found in the crystal structures (represented by  $\gamma$  and  $h_M$  in Table I).

The one-electron energy of a model system  $[Cl(H)_2Cu(\mu\text{-ox})Cu(H)_2Cl]^{4+}$  in its singlet and triplet configurations is plotted as a function of  $\gamma$  in Figure 5a, showing minima at  $27^\circ$  for both cases. A similar result is obtained for a system with one less electron per metal atom, a crude model for analogous Ni(II) complexes, with an energy minimum for the singlet at  $\gamma = 20^\circ$ . In Figure 5b, we plot the energy of the  $\sigma^*(M-L_{ax})$  orbital as a function of the bending angle. There it can be seen that the reason for stabilization upon bending is the improved overlap between the acceptor orbitals 9a and the apical  $\sigma$ -donor orbital. At the

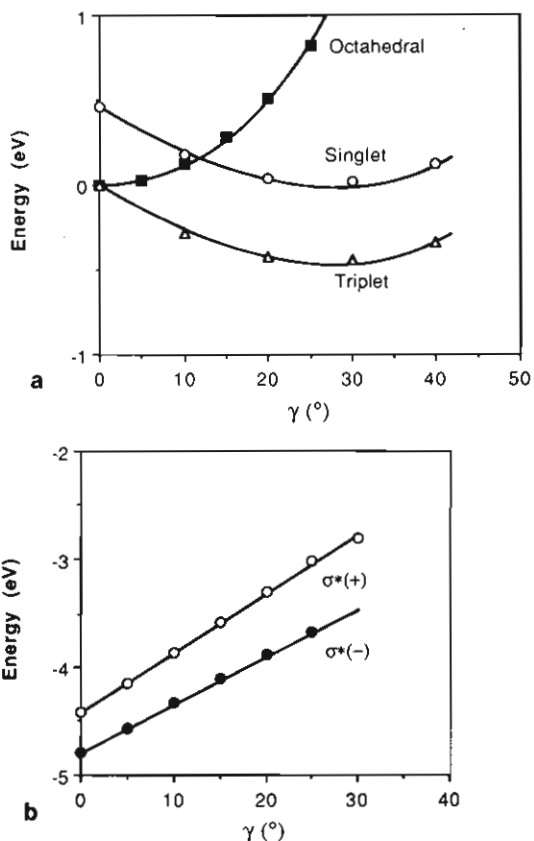


**Figure 5.** (a) Total one-electron energy as a function of bending  $\gamma$  for a model dinuclear compound  $[Cl(H)_2Cu(\mu\text{-C}_2\text{O}_4)Cu(H)_2Cl]^{4+}$  in its singlet and triplet configurations. Also the energy of a bis-octahedral compound  $[Cl_2(H)_2Cu(\mu\text{-C}_2\text{O}_4)Cu(H)_2Cl_2]^{6+}$  is shown. The zero of energy has been arbitrarily chosen in each case. (b) Walsh diagram for the in-phase (+) and out-of-phase (-) combinations of the  $\sigma^*(M-L_{ax})$  orbitals of the former model compound.

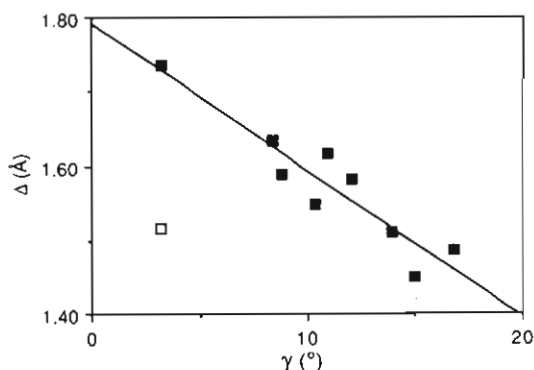


**Figure 6.** Plot of the difference between the axial bond distance Cu-X and the X covalent radius ( $\Delta$ ) as a function of the bending angle  $\gamma$  for the oxalato-bridged compounds in Table I. For those compounds with two axial ligands, only the shortest Cu-X distance has been taken into account.

same time, the  $p_z/d_{z^2}$  hybridization decreases the destabilizing interaction of the  $d_{z^2}$  lone pairs 9b with the apical donors'  $\sigma$  lone pairs.

In Figure 6, one can find the experimental counterpart of our theoretical analysis of bending. There, we plot the difference between the Cu-X bond distance and the covalent radius of X<sup>39</sup> vs the bending angle  $\gamma$  for the oxalato-bridged compounds. Only one out of ten independent data sets in Table I deviates significantly from the expected trend: the larger the bending of the basal plane, the stronger the Cu-X bond. The degree of bending and

(38) For a discussion on the pyramidalization of the metal atom in square pyramidal complexes, see, e.g.: Rossi, A. R.; Hoffmann, R. *Inorg. Chem.* 1975, 14, 365.

(39) Huheey, E. J. *Inorganic Chemistry*, 3rd ed.; Harper and Row: New York, 1983.

the axial bond distance are also well correlated with the out-of-plane displacement of the Cu atom (not shown in Figure 6).

Association of a sixth ligand would introduce a poor bonding interaction with the acceptor orbitals **9a** but a strong interaction with the occupied orbitals **9b**, explaining the long bonding distance for the sixth ligand in the case of pseudooctahedral compounds (axial distances<sup>6</sup> in the perchlorate, M–O = 2.348 and 2.341 Å for the fifth ligand and 2.766 and 2.703 Å for the sixth ligand; in the hexafluorophosphate, M–F = 2.445 and 2.756 Å). **9b** also suggests that the copper atoms may act as donors through the  $d_{z^2}$  orbitals and form a bond to a Lewis acid in the sixth coordination position. There are precedents for similar interactions in  $d^8$  compounds in which a Pt(II) atom in a square-planar environment is bound to  $Tl^+$  or  $K^+$  ions<sup>40</sup> or to an  $AgL^+$  fragment,<sup>41</sup> but we are not aware of such interactions in  $d^9$  complexes.

In contrast to the twisting distortion discussed above, the bending motion is related to metal–axial-ligand interactions and consequently is not expected to depend on the nature of the bridging ligand. By comparing data in Tables I and II one can see that a significant bending appears for most square-pyramidal complexes, as well as for hexacoordinate complexes with markedly different axial ligands, regardless of the nature of the bridging ligand.

### Effect of Bending on the Magnetic Exchange

Several theoretical studies have provided a rationale for the changes in the magnetic coupling constants within families of related dinuclear Cu(II) compounds. However, those studies have focused on square-planar complexes and on geometrical parameters other than the bending around the O–O hinge discussed in the previous section. In the following, we briefly describe the theoretical background for a qualitative analysis of the magnetic exchange at the one-electron level and discuss then the results.

For Cu(II) dinuclear complexes, the magnetic coupling constant  $J$  is directly related to the energy separation between the singlet and triplet states (eq 7). A perturbative treatment of the con-

$$2J = \epsilon_S - \epsilon_T \quad (7)$$

figuration interaction problem was developed by de Loth et al.,<sup>42</sup> which results in the following expression for  $J$ :

$$2J = 2K_{ab} - \frac{(\epsilon_1 - \epsilon_2)^2}{J_{aa} - J_{ab}} + \text{other terms} \quad (8)$$

In this equation,  $\epsilon_1$  and  $\epsilon_2$  are the SCF energies of the two partially occupied molecular orbitals (HOMO and LUMO); the a and b indices refer to localized orbitals obtained by appropriate combinations of the HOMO and LUMO, and  $K_{ab}$ ,  $J_{aa}$ , and  $J_{ab}$  are the corresponding exchange and Coulomb integrals. The first term in eq 8 (the "potential exchange") is always positive. The second term, referred to as "superexchange" or "kinetic exchange", is always negative. There are more second- and fourth-order terms not shown explicitly in eq 8, which are usually negative.

Several authors have carried out ab initio calculations on dinuclear Cu(II) complexes, with different bridging ligands.<sup>42–45</sup> In general, the important contributions to  $J$  come from the two terms made explicit in eq 8, although the other ones are not negligible. A careful analysis of the different contributions to  $J$  shows that the potential exchange plus the other terms add up to a negative value that is typically less than 20% of the superexchange contribution (35% in the worse case). More important

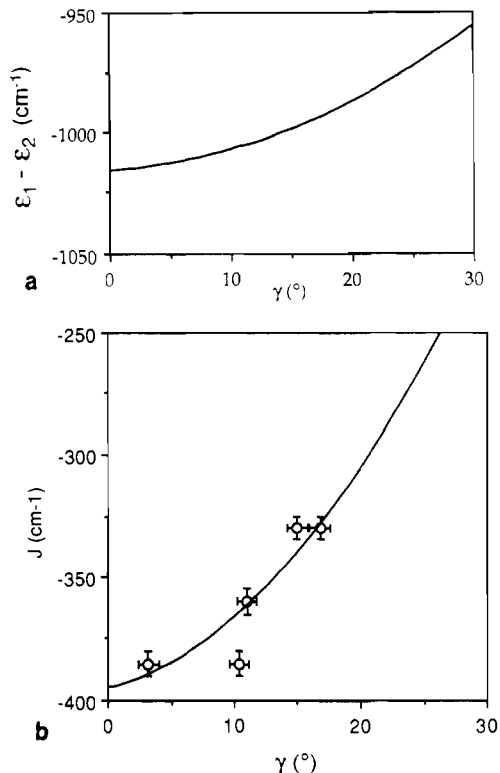


**Figure 7.** Dependence of the antiferromagnetic coupling constant  $J$  on the bending angle  $\gamma$ : (a) calculated ( $\epsilon_1 - \epsilon_2$ ) for the model compound  $[Cl(H)_2Cu(\mu-C_2O_4)Cu(H)_2Cl]^+$ ; (b) experimental values for a family of six oxalato-bridged dinuclear complexes with bpy or phen as terminal ligands (see Table I) as a function of  $\gamma$  (the error bars for  $\gamma$  and  $J$  are set arbitrarily to  $1^\circ$  and  $5 \text{ cm}^{-1}$ , respectively).

for our study is the fact that the variations of the calculated  $J$  upon geometry changes<sup>44,45</sup> nicely follow the changes in the superexchange contribution. Hence we can obtain a rough estimate of the geometry dependence of  $J$  by calculating orbital energies,  $\epsilon_1$  and  $\epsilon_2$ , at the extended Hückel level, and assuming the Coulomb term ( $J_{aa} - J_{ab}$ ) to be approximately unchanged by geometry changes.

Let us go back to our model compound  $[Cl(H)_2Cu(\mu-ox)Cu(H)_2Cl]^+$  and see what happens to the energies of the HOMO and the LUMO when the molecule is bent around the O–O hinge. In fact, changes in the overlap between  $d_{xy}(\text{Cu})$  and the oxalato orbitals of symmetry  $b_{1g}$  and  $b_{2u}$  (**4**) are small and almost parallel. As a result, the term  $(\epsilon_1 - \epsilon_2)$  shows only a small variation upon bending (Figure 7a), in excellent agreement with the small range of experimental coupling constants ( $-402 < J < -330 \text{ cm}^{-1}$ ) as compared to those found for hydroxo- or alkoxo-bridged copper(II) dinuclear complexes<sup>46</sup> as a function of the Cu–O–Cu angle ( $-400 < J < +100 \text{ cm}^{-1}$ ).

If one focuses on the fine details, it is found that  $(\epsilon_1 - \epsilon_2)^2$  increases with  $\gamma$ . This result can be traced back to the differences in hybridization of the  $b_{1g}$  and  $b_{2u}$  orbitals of the oxalato ligand. The overlap of  $d_{xy}(\text{Cu})$  with  $p_y$  of the oxygen atoms is insensitive to the bending motion, while its overlap with  $p_x$  is maximum at  $\gamma = 0^\circ$  and drops to zero at  $\gamma = 90^\circ$ . Now,  $b_{2u}$  has approximately equal contributions ( $0.36p_x$ ,  $0.35p_y$ ) from both oxygen atomic orbitals, whereas  $b_{1g}$  has more  $p_y$  character ( $0.16p_x$ ,  $0.46p_y$ ). It is thus clear that  $b_{2u}$  loses more overlap than  $b_{1g}$  and becomes less antibonding, therefore increasing their separation as  $\gamma$  is increased. The experimental values of  $J$  for a family of analogous compounds, having bpy or phen as terminal ligands, are shown in Figure 7b and nicely correlate with the theoretical predictions. Given the differences in the number and nature of the axial ligands along this family, the correlation found between  $J$  and  $\gamma$  is remarkable. The curve shown in Figure 7b was obtained by a linear fitting of the experimental values of  $J$  to the orbital energy differences

(40) (a) Nagle, J. K.; Balch, A. L.; Olmstead, M. M. *J. Am. Chem. Soc.* **1988**, *110*, 319. (b) Olsson, L.-F.; Oskarsson, A. *Acta Chem. Scand.* **1989**, *43*, 811.

(41) Usón, R.; Forniés, J.; Tomás, M.; Casas, J. M. *Angew. Chem., Int. Ed. Engl.* **1989**, *28*, 748.

(42) de Loth, P.; Cassoux, P.; Daudey, J. P.; Malrieu, J. P. *J. Am. Chem. Soc.* **1981**, *103*, 4007.

(43) Charlot, M. F.; Verdager, M.; Journaux, Y.; de Loth, P.; Daudey, J. P. *Inorg. Chem.* **1984**, *23*, 3802.

(44) Astheimer, H.; Haase, W. *J. Chem. Phys.* **1986**, *85*, 1427.

(45) Handa, M.; Koga, N.; Kida, S. *Bull. Chem. Soc. Jpn.* **1988**, *61*, 3853.

(46) Willett, R. D. In ref 2, p 289.

**Table III.** Orbital Exponents (Contraction Coefficients of Double- $\zeta$  Expansion Given in Parentheses) and Energies Used in the Extended Hückel Calculations

atom	orbital	$\zeta_i (c_i)$	$H_{ii}, eV$
Cu	4s	2.20	-11.40
	4p	2.20	-6.06
	3d	5.95 (0.5770), 2.10 (0.6168)	-14.00
S	3s	1.817	-20.00
	3p	1.817	-13.30
Cl	3s	2.033	-30.0
	3p	2.033	-15.0
O	2s	2.275	-32.30
	2p	2.275	-14.80

$(\epsilon_1 - \epsilon_2)^2$ . Neglecting the "other terms" and introducing the fitting parameters in eq 8, we obtain semiempirical estimates of the two-electron terms  $K_{ab} = 1196 \text{ cm}^{-1}$  and  $J_{aa} - J_{ab} = 324 \text{ cm}^{-1}$ , to be compared with the ab initio value  $K_{ab} = 720 \text{ cm}^{-1}$  calculated by Charlot et al.<sup>43</sup> for an oxalato-bridged dinuclear compound.

### Concluding Remarks

The extent of the twisting distortion ( $\alpha$ ) in Cu(II) dinuclear complexes with  $C_2X_4$  bridging ligands is found to depend on the nature of the X atoms: the less electronegative X is, the greater the importance of the distortion is. Inclusion of the  $C_2X_4$  fragment into a larger ligand, as in bipyrimidine or benzoquinone, reduces the extent of the distortion. For the analogous Ni(II) complexes with one less electron per metal atom, the planar structure is preferred.

The driving force for the bending of the basal plane of the metal relative to the plane of the  $C_2X_4$  bridge is the strengthening of

the metal-axial-ligand bond, for both Cu(II) and Ni(II) complexes. According to this conclusion, when two equivalent axial ligands are present, no bending occurs. This bending has a small effect on the magnetic exchange interactions: the magnetic coupling becomes less antiferromagnetic when the bending angle  $\gamma$  is increased.

**Acknowledgment.** Financial support of this work was generously given by CICYT through Grants PB86-0272 (Barcelona) and PB88-0490 (València). We are grateful to G. De Munno, J. Ribas, and A. Gleizes for facilitating unpublished data and to J. J. Novoa and P. Alemany for discussions.

### Appendix: Computational Details

The qualitative theoretical discussions in this paper are substantiated by molecular orbital calculations of the extended Hückel type<sup>47</sup> with a modified Wolfsberg-Helmholz formula.<sup>48</sup> Atomic parameters used are shown in Table III.<sup>3,47</sup>

Calculations were performed for the following model complexes: (A)  $[(H)_2Cu(\mu-C_2O_4)Cu(H)_2]^{n-}$  ( $n = 2, 0$ ); (B)  $[Cl(H)_2Cu(\mu-C_2O_4)Cu(H)_2Cl]^{n-}$  ( $n = 4, 2$ ); (C)  $[(H)_2Cu(\mu-C_2S_4)Cu(H)_2]^{2-}$ ; (D)  $[(H)_2Cu(\mu-5)Cu(H)_2]^{2-}$ ; (E)  $[(H)_2Cu(\mu-6)Cu(H)_2]^{n-}$ . Bond distances (Å) and angles used for A and B: Cu-O = 2.00, Cu-H = 1.70, Cu-Cl = 2.60, C-C = 1.54, C-O = 1.25; CCO = 117, HCuH = 90°. Bond distances (Å) and angles (deg) used for C: Cu-S = 2.26, Cu-H = 1.80, C-C = 1.47, C-S = 1.70; CCS = 120. Bond distances (Å) and angles (deg) used for D and E: Cu-O = 1.95, Cu-N = 2.00, C-C(ring) = 1.37, C-C(inter-ring) = 1.47, C-N = 1.37, C-H = 1.08; CCO = 115, ring angles = 120.

(47) Hoffmann, R. *J. Chem. Phys.* **1963**, *39*, 1397.

(48) Ammeter, J. H.; Bürgi, H.-B.; Thibault, J. C.; Hoffmann, R. *J. Am. Chem. Soc.* **1978**, *100*, 3686.

Contribution from the Monsanto Company,  
St. Louis, Missouri 63167

## Oxygen-Stable Ferrocene Reference Electrodes<sup>1</sup>

James K. Bashkin\* and Patrick J. Kinlen

Received February 14, 1990

Reference electrodes (RE's) play an important role in electrochemistry, but standard designs suffer from limitations. Ferrocene derivatives have been reported to serve as alternative RE's, but they suffer from poor stability to oxygen, water, and nonaqueous solvents. The previously described ferrocene-based RE's are unstable due to the reaction of ferrocenium ion ( $Fc^+$ ) with dioxygen. We have found that sufficient methyl substitution of the cyclopentadienyl rings can render ferrocenium stable to  $O_2$ , and ring-methylated  $Fc^+$  analogues may be used to fabricate stable RE's. A bis(pentamethylcyclopentadienyl)iron reference electrode is described; its potential is pH independent in aqueous buffer solutions. Unlike any other ferrocene electrodes previously reported, these electrodes are stable in aqueous solvents in air. A new reference standard for use under aerobic conditions is proposed.

Reference electrodes (RE's) are ubiquitous in electrochemistry, being necessary components of pH probes and other electrochemical sensors. Commonly used reference electrodes (e.g., the saturated calomel electrode (SCE) or the silver/silver chloride electrode) contain an aqueous internal filling solution. At high pressures, the solution being tested may leak back into the reference electrode compartment, contaminating the internal reference solution. This problem may be eliminated by internal pressurization of the reference electrode, but this significantly complicates electrode design and increases cost. In addition, aqueous reference electrodes are not well-suited for use in nonaqueous solvents, since unknown and irreproducible liquid-junction potentials exist between the aqueous and nonaqueous phases. Furthermore, contamination of the sample by water and other ions associated with the reference electrode may occur. For nonaqueous electrochemistry, IUPAC recommends<sup>2</sup> the use of a redox couple such as ferrocene/ferrocenium ion ( $Fc/Fc^+$ ) as

an internal standard. The  $Fc/Fc^+$  couple is an appropriate choice because its potential is largely independent of the solvent.

An alternative to the liquid junction electrode is one based on an entirely solid-state design. Peerce and Bard<sup>3</sup> elegantly fabricated such an electrode by coating poly(vinylferrocene) (PVFc) on platinum. The polymer-coated electrode was brought to a 1:1 ratio of ferrocene to ferrocenium by poisoning the electrode at the PVFc/ $Fc^+$  half-wave potential (0.39 V vs SCE). Although this electrode maintained a constant, reproducible potential in deaerated acetonitrile over 21 h, it was unstable in other nonaqueous solvents, including benzonitrile, DMF, and methanol. The electrode's rapid potential drift in these solvents was attributed to gradual dissolution of PVFc<sup>+</sup>, and it was predicted that higher molecular weight PVFc should be more useful in a wide range of solvents. In aqueous solution, the potential of the PVFc electrode drifted 150 mV overnight, even with deaeration.

Cross-linking strategies for PVFc were employed by Kannuck and co-workers<sup>4</sup> to prepare RE's with no solubility problems, but

(1) Bashkin, J. K.; Kinlen, P. J. U.S. Patent 4,857,167, 1989.

(2) (a) Gritzner, G.; Kuta, J. *Pure Appl. Chem.* **1984**, *56*, 461-6. See also: (b) Gagné, R. R.; Koval, C. A.; Lisensky, G. C. *Inorg. Chem.* **1980**, *19*, 2854-5. (c) Bond, A. M.; McLennan, E. A.; Stojanovic, F. G.; Thomas, F. G. *Anal. Chem.* **1987**, *59*, 2853-60.

(3) Peerce, P. J.; Bard, A. J. *J. Electroanal. Chem. Interfacial Electrochem.* **1980**, *108*, 121-5.

(4) Kannuck, R. M.; Bellama, J. M.; Blubaugh, E. A.; Durst, R. A. *Anal. Chem.* **1987**, *59*, 1473-5.